Structure and Dynamics of Hydrogen Bonds in the Interface of a C 12 E 6 Spherical Micelle in Water Solution: A MD Study at Various Temperatures

ARTICLE *in* THE JOURNAL OF PHYSICAL CHEMISTRY B · OCTOBER 2006

Impact Factor: 3.3 · DOI: 10.1021/jp0602070 · Source: PubMed

4 AUTHORS, INCLUDING:

Fabio Sterpone
French National Centre for Scientific Research
46 PUBLICATIONS **1,047** CITATIONS
SEE PROFILE

Giuseppe Briganti
Sapienza University of Rome
58 PUBLICATIONS **803** CITATIONS
SEE PROFILE

Structure and Dynamics of Hydrogen Bonds in the Interface of a $C_{12}E_6$ Spherical Micelle in Water Solution: A MD Study at Various Temperatures

Fabio Sterpone,*,†,‖ Carlo Pierleoni,‡ Giuseppe Briganti,§ and Massimo Marchi⊥

University of Texas at Austin, Departement of Chemistry and Biochemistry, University Station 1, CM A 5300 Austin, TX, 78712, and INFM CRS-SOFT and Physics Department, University of L'Aquila, Italy, and INFM CRS-SOFT and Dipartimento di Fisica, Università di Roma "La Sapienza", P.A.Moro 2, 00185 Roma, Italy, and [4]Commissariat à l'Energie Atomique, DSV-DBJC-SBFM, Centre d'Études, Saclay, 91191 Gif-sur-Yvette Cedex, France

Received: January 11, 2006; In Final Form: July 13, 2006

The temperature dehydration of a $C_{12}E_6$ spherical micelle is characterized through the study of the structure and dynamics of the hydrogen bonds formed by water within the micellar interface. Water molecules in proximity of the hydrophilic fragment of the $C_{12}E_6$ surfactants form strong H-bonds with the oxyethilene units *E* and with the polar alcoholic heads. The activation energies of such H-bonds fall in the range 2−3 Kcal mol^{-1}. On the exposed oil core, the number of water−water H-bonds decreases as an effect of dehydration. The dynamics of such bonds exhibits a slow relaxation with respect to the bulk, and two time scales can be discerned: the first one, $\tau \simeq 3-6$ ps, is typical of water−water H-bonds around small hydrophobic molecules, whereas the second one, $\tau \simeq 40-80$ ps, is probably due to the confining effect of the long hydrophilic fragments which reduces the probability of a water molecule to leave the hydration layer of the exposed oil core. Water molecules around the core form H-bond clusters whose size and distribution change with temperature. From a cluster analysis, the system appears to be below the percolation threshold, suggesting that the exposed oily surface is formed by disconnected patches of size around 1 nm^2, close to the estimate of the solvated hydrophobic patches on protein surfaces. The network connectivity is also considered for concentric hydration shells along the interface: it turns out that near the oil core, the cluster size is larger than elsewhere in the interface demonstrating a strong structural effect induced by the exposed hydrocarbon tails. Temperature affects the cluster size only in the innermost shell.

1. Introduction

The structural and thermodynamic properties of surfactants in aqueous solutions depend on the competing interactions of water with the hydrophobic and hydrophilic moieties constituting the monomeric chain. In certain thermodynamics conditions, and above the critical micellar concentration (CMC), they form aggregates of different shapes and sizes.[1] The hydration state of a micelle, defined as the amount of water confined in the interfacial region between the oil core and the bulk solution, is considered a key parameter to understand the shape, size, and size distribution of such aggregates in water. For this reason, several experimental techniques have been used to quantify the micelle hydration state. Data were collected from light scattering, dielectric and ultrasonic relaxation, density increment, small angle neutron scattering, and heavy aggregate diffusion by means of NMR and ^{17}O magnetic relaxation.[2] Unfortunately each experimental technique gives hydration numbers which depend on the specific model used to evaluate the contrast between the interfacial and bulk water molecules. However a general behavior has been observed for almost all surfactants studied: the degree of hydration of the micelles decreases upon increasing the temperature.

In the case of the non ionic C_iE_j micelles, two experiments have provided a local definition of the hydration in C_iE_j micellar interface: from a cell-diffusion analysis of the D_2O diffusion in a low concentration $C_{12}E_8/D_2O$ solution, Jönstromer et al.[2] have shown that the hydration state of a spherical micelle increases strongly along the direction normal to the oil core surface. As a consequence, the interface can be separated in an inner region−close to the oily core−and an outer region with a different amount of water molecules for *E* units. Furthermore, these experiments indicate that temperature dehydration mainly arises from the water molecules within the inner region. The different temperature response of hydration water in the inner and outer region of the interface has been confirmed by a new experimental technique, known as *chemical trapping*.[3,4] Exploiting the reactivity of a chemical probe incorporated in the micellar structure, Romsted and Yao have measured, at various temperatures, the quantity of water molecules in the interfacial region of holomicelles ($C_{12}E_6$) and mixed micelles of C_iE_j. They found that dehydration occurs mainly in the inner shell of the interface where the probe is localized. Molecular dynamics (MD) simulations of a spherical $C_{12}E_6$ micelle in a water solution at different temperatures have supported these experimental findings.[5] Simulations have shown that the number of water molecules per *E* unit increases along the interface $N_w(R) \sim R^2$, and temperature dehydration occurs just in the first two internal shells, in agreement with the Romsted and Yao results.

* Corresponding author phone: +39-6-444861; fax: +39-6-4957083; e-mail: f.sterponeecaspur.it.
† University of Texas at Austin.
‡ University of L'Aquila.
§ Università di Roma.
⊥ Commissariat à l'Energie Atomique.
‖ Current address: Caspur, Via dei Tizii, 6/6 - 00185 Rome, Italy.

10.1021/jp0602070 CCC: $33.50
Published on Web 08/30/2006

With a more local analysis, based on the Voronoi tassellation of the aggregate surface exposed to solvent, it was found that the hydration number, defined now as the number of water molecules in contact with the solute, both the hydrophilic groups and oil core, decreases as an effect of the temperature change; however, the percentage decrease is larger for the oil core (8%) than for the *E* units (0.8%). We should mention, however, that a different view of temperature dehydration related to conformational changes of the *E* units has been proposed.[6,7] Theoretical models[6] and experiments[7] suggest that the trans state of the CC torsion in the *E* units becomes more stable when the temperature is increased and this induces a larger screening to water of the hydrophilic moieties.

The study of the hydration water along the micellar interface, namely in proximity of the exposed oil core and the hydrophilic moieties, is crucial for characterizing the dehydration phenomena. Moreover this study allows us also to tackle two topical problems in the understanding of hydration water around biomolecules: the effect of hydrophobic regions of subnanometer size and the effect of geometrical confinement. The non uniform distribution of the hydrophilic terminations in the interface of the $C_{12}E_6$ implies the presence of separated hydrophobic patches exposed to the solvent. As we will estimate in the following, the average size of a single patch is of the order of 1 nm^2 and the total size of exposed hydrophobic surface is roughly 30 nm^2, which is 30% of the total surface of the micelle exposed to the solvent. Thus a $C_{12}E_6$ spherical micelle represents an interesting model to gain insight into the structural effects induced on water by non-extended hydrophobic regions, as those present in biomolecules. In monomeric proteins, the hydrophobic regions account for 50−55% of the total accessible surface,[8] their size is about 1−6 nm^2, and they alternate on the surface to hydrophilic regions. The water structure and dynamics around such hydrophobic regions play an important role for protein function, folding, and structure, but it is still not completely understood, although important results are now available.[9,10] Recently, in order to simplify, the behavior of water around flat hydrobobic/hydrophilic surfaces has been studied providing information about dewetting processes and the structural properties of water.[11,12] Furthermore, in contrast to most of the isolated biomolecules in the water solution, the interfacial water of a $C_{12}E_6$ micelle experiences a geometrical confinement due to the long hydrophilic tails. The characterization of such a confinement can be important for understanding water behavior in more complex situations such as protein−protein or protein/surface interactions.

In general, the analysis of the solvation of biomolecules have focused on single molecule properties, such as diffusion, dipolar relaxation, local orientation, or single H-bond distribution and dynamics. To our knowledge, very few works[13,14] have studied the spatial extension of such structural properties, for example, considering the size and distribution of the H-Bond network formed by water around a protein. However, as demonstrated by recent studies of water in confined environments (carbon nanotube, hydrophobic plates, hydrophobic pockets),[15−18] the structure and size of the cluster is crucial for understanding the effect of the hydrophobic interaction.

In this paper, we present a detailed MD study of the structural and dynamic properties of the hydrogen bonds formed by water along the thick interface of a spherical $C_{12}E_6$ micelle at various temperatures. In particular, we focus on the structure, connectivity, and dynamics of the water in the vicinity of the hydrophobic surface and the hydrophilic fragments of the surfactants. In addition, we present a cluster analysis of the connectivity of the hydration water around the hydrophobic core and along the thick interface.

The article is organized as follows: In section 2, we describe the force field and the MD simulation protocol. In section 3, the hydrogen bonds between the solvent and the hydrophilic part are analyzed to quantify the stability of *E*-water interactions. Then, in section 4, we focus on the oil core surface exposed to the solvent. The water−water H-bonds near the core are then computed, and their dynamical relaxation derived. The networks of water−water H-bonds are also characterized. Finally, in section 5, we study the H-bond network in the framework of the shell analysis of reference.[5]

2. Methods

2.1. Systems and Force Field. The system consists of a spherical micelle formed by 45 $C_{12}E_6$ monomers and 8448 water molecules. The system is simulated in a truncated octahedral cell of initial linear dimensions, $L_x = L_y = L_z = 84$ Å. An all-atom force field describes the interactions between the constituents of the system (see the details in ref 19): The parameters for the hydrophilic moiety (E_6 or PEO in the following) are taken from Tasaki,[20] the alcoholic termination is described by the Charmm22 force field,[21] and the hydrocarbon tail is modeled by a potential model developed by Tobias et al. for alkanes[22] and used to model the hydrocarbon tail of lipids.[23] In our model all the bond lengths of the surfactant are fixed at the equilibrium value by the constraints method,[24] thus the chain is partially flexible. Coherently with the force field for PEO, the simple point charge model (SPC) describes water molecules.

The van der Waals interactions are represented by a 12-6 Lennard-Jones potential.[20,23] When different force fields are combined, the geometrical combination rules for the coefficients of the potential have been applied. For the hydrocarbon tail, following the prescription of original works,[22,23] we excluded the 1-4 interactions.

2.2. MD Protocols. The $C_{12}E_6$ micelle was simulated in the NPT ensemble[25] at six temperatures, $T = 5°$, 10°, 15 °C and $T = 40°$, 45°, 50 °C, and at a pressure $P = 1$ atm. The thermostat and barostat characteristic times were fixed to $\tau_T = 0.4$ ps and $\tau_P = 4$ ps, respectively. For this system, a single time step of $\tau = 1$ fs was used to numerically integrate the dynamics of the system. The electrostatic energy was evaluated by employing the SPME scheme[26] with the following parameters: $\alpha = 0.33$ Å^{-1}, $n_x = n_y = n_z = 60$ grid points, and β-spline order $n = 4$. Non-bonded L−J and direct space electrostatic interactions were truncated at the cutoff $r_c = 9$ Å. We run four and eight independent trajectories at $T = 10$ °C and $T = 45$ °C, respectively. The single run was 300 ps long at $T = 10$ °C, and 250 ps at $T = 45$ °C. For each of the supplementary trajectories at $T = 5$ °C, 15 °C, 40 °C, 50 °C, four independent trajectories of 250 ps were run. In all cases, configurations were stored every 200 fs. Time correlation functions were extracted over the independent trajectories and then averaged together for each fixed temperature.

All the simulations were carried out using the DLPROTEIN package, modified to run parallel independent simulations on a Linux cluster.

3. Water-PEO Hydrogen Bonds

The relationship between water dynamics and hydrogen bonds structure and connectivity at the micellar interface has been already studied fruitfully in the case of cesium pentadecafluorooctanoate micelle (CsPFO) by Pal et al.[27,28] It was shown that

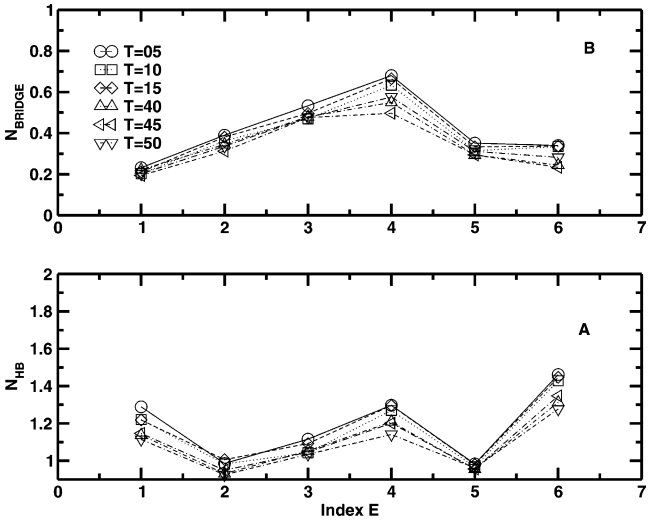

Figure 1. Hydrogen bonds along the PEO. Panel A: number of water H-bonded per E unit. Panel B: number of water molecules connecting two oxygens of different E units in the same monomer.

the bonded water molecules contribute to slow the water dynamics at the interface, being the H-bonds formed by water with the surfactant stronger and more persistent than those between two water molecules in the bulk. It was also demonstrated that water at the interface can be classified depending on the H-Bond type formed with the surfactant, namely water single bonded, water bridging two different monomers, and free water molecules. The average water dynamics at the micellar interface was considered as the result of a dynamical equilibrium among these types of water molecules and the bulk.

In the following, we want to study the water H-Bond connectivity with the hydrophilic units of the $C_{12}E_6$ micelle. The helical folded structure of PEO in water solution has been extensively studied in the past by experiments, theory, and simulations.[20,29−32] From simulations at low concentration, it appears that water molecules stabilize the helical structure of PEO bridging the oxygens of alternate *E* units:[20] $E_{i+2} - E_i$. In C_iE_j spherical micelles,[19,5] as well as in bilayers[33] or monolayers[34] and in reverse micelles,[35] the hydrophilic moiety, constituted by *j E* units, similarly folds in a helical structure. Moreover, in such aggregates, the oxyethylene units belonging to different monomers effectively attract each other, with an interaction strength that depends on the degree of hydration.

As known from previous simulations of a $C_{12}E_6$ spherical micelle[5] the hydration state of the hydrophilic part, is almost unchanged upon increasing the temperature from $T = 10$ °C to $T = 45$ °C: The number of water molecules in contact with the *E* units decreases about 0.8%. Recently, the dynamics of water in the proximity of the micelle has been also investigated;[36] it turns out that at low ($T = 10$ °C) and high ($T = 45$ °C) temperatures, the set of water molecules around the hydrophilic fragment is characterized by retarded translational diffusion compared to that in pure water solution. Because of the structure of water along the hydrophilic chains, the rotational relaxation is strongly retarded too. To better understand these results, the structure and dynamics of the water−PEO H-bonds[37] is considered here.

3.1. Structure of W−PEO H-Bonds. In Figure 1, for each *E* unit along the single $C_{12}E_6$ surfactant ($E = 1$ refers to the innermost unit), we show the number of hydrogen bonds formed with water (panel A) and the number of water molecules connecting two oxygens in the same monomer (N_{bridge} in panel B). Comparing panels A and B, we observe that only a portion of water molecules H-bonded to the hydrophilic fragments are also double-bonded with another *E* unit of the same chain. The portion of water forming internal bridges, $p = N_{bridge}/N_{hb}$, is around 50% for central units ($E = 4$ and $E = 3$) and decreases for the external units ($p \simeq 20-30\%$ for $E = 2 = 5 = 6$ and less for $E = 1$). Indeed, the highest number of bridges is found at unit $E = 4$ where there are connections forward and backward to $E = 6$ and $E = 2$, respectively. Unit $E = 3$, which can be connected to $E = 5$ and $E = 1$, has a smaller number of H-bond bridges, showing that, in our system, the helix is only partially formed. The lack of bridges in the internal *E* units can be related to the perturbation due to the anchoring with the alkyl tail. The temperature changes the above distribution slightly. The greatest effects concern units $E = 1$, $E = 4$, and $E = 6$, which lose almost 15 H-bonds from $T = 10$ °C to $T = 45$ °C. Consequently, units $E = 4$ and $E = 6$ have a lower number of water bridges ($\simeq -20\% \div -30\%$), so that the hydrophilic fragments are less structured.[38] As global effect of the temperature increase, the total number of hydrogen bonds formed by water and the *E* units decreases from 310 ($T = 10$ °C) to 297 ($T = 45$ °C). Single-molecule bridges connecting two different monomers, although rare, are also observed (data not shown), they are located at the inner unit and their number, surprisingly, increases with temperatures.

3.2. Dynamics of W−PEO H-Bonds. H-bonds dynamics is studied by computing the correlation function:[39]

$$C(t) = \langle h_i(t)h_i(0)\rangle/\langle h_i(0)h_i(0)\rangle \qquad (1)$$

where the function $h_i(t)$ takes the value 1 if the tagged *i*th H-bond is present at time *t*, the value of 0 otherwise. Since the memory of what happens in the interval *t* is not included in such a definition, the $C(t)$ function yields the probability of destroying and reforming a given H-bond as a function of time.

The H-bonds formed by water with the hydrophilic fragments can be divided in three categories (see top panel of Figure 2):

(1) water H-bonding with the oxygen of the *E* unit (W_H-E).

(2) water H-bonding with the oxygen of the alcoholic head (W_H-Alc).

(3) water accepting hydrogen bond from the alcoholic head (W_O-Alc).

Figure 2 shows the behavior of $C(t)$ for the three different types of H-bonds at $T = 10$ °C and for the water−water hydrogen bond computed for all the solvent molecules of the solution. The correlation functions are fitted in order to evaluate the hydrogen bond lifetime $\langle\tau_{hb}\rangle$ as the integral of the $C(t)$. Results at different temperatures are reported in Table 1. For W_H-E and W_O-Alc the $C(t)$s decay is well fitted by a stretched exponential, while for the W_H-Alc, a linear combination of a stretched exponential and a simple exponential function is needed. As a general feature, the lifetimes $\langle\tau_{hb}\rangle$ at $T = 10$ °C are 2 times larger than those at $T = 45$ °C. The H-bonds formed by water and the *E* units are the most stable with lifetimes of $\langle\tau_{hb}\rangle = 117.7$ ps and $\langle\tau_{hb}\rangle = 51.2$ ps at $T = 10$ °C and $T = 45$ °C, respectively, while between those formed by water and the alcoholic head, the W_O-Alc bond ($\langle\tau_{hb}\rangle = 96.1$ ps at $T = 10$ °C and $\langle\tau_{hb}\rangle = 39.7$ ps at $T = 45$ °C) survives longer than the others whose lifetime is on the order of few picoseconds. All these lifetimes are larger than the characteristic time of the bulk water−water H-bond (see bottom panel of Figure 2).

The disruption of a hydrogen bond can be viewed as a bound-to-free state transition, so that by the application of transition state theory, we can derive the activation energy

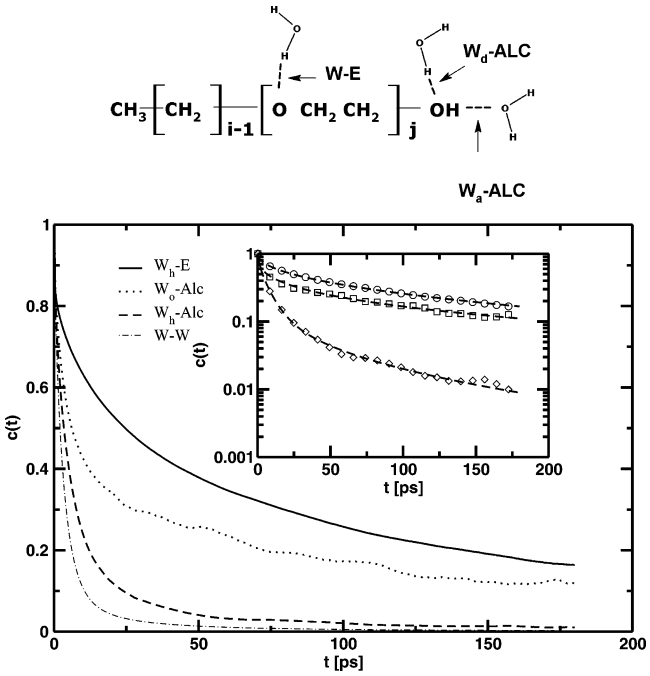

Figure 2. Top: schematic view of the hydrogen bonds formed by water molecules with the hydrophilic fragment of the surfactanct C_iE_j. Bottom: correlation functions $C(t)$s at $T = 10$ °C for the three types of hydrogen bonds formed by water with the hydrophilic fragment and for water−water hydrogen bond computed in the solution. We report with the dashed line the $C(t)$ for the hydrogen bonds formed between water and the alcoholic head being water the hydrogen donor, with the dotted line the $C(t)$ for hydrogen bonds between water and the alcoholic head being water the hydrogen acceptor, and with the solid line the $C(t)$ for hydrogen bonds between water and the oxygen of the E unit. With the dotted−dashed line, we report the $C(t)$ for the hydrogen bond formed between water molecules in the entire solution. In the inset graph (linearlog) the fit of the three correlation functions associated to the water−PEO H-bonds are presented with the dashed line.

TABLE 1: Characteristic Times Extracted by Fitting the *C*(*t*) Correlation Function for Different Types of Hydrogen-bond.[a]

hydrogen bond $T = 10$ °C	τ_s [ps]	τ_e [ps]
W_h-E	117.7	
W_o-Alc	96.1	
W_h-Alc	9.6	7.1
hydrogen bond $T = 45$ °C	τ_s	τ_e
W_h-E	51.2	
W_o-Alc	39.7	
W_h-Alc	2.5	4.1

[a] For W_h-E and W_o-Alc, the fit is performed using a single stretched exponential. In the case of W_h-Alc, we use a combination of a stretched exponential and a simple exponential

E_A for any given type of H-bond:[40]

$$\frac{1}{\langle \tau_{hb} \rangle} = \frac{k_b T}{h} e^{-E_A/k_b T} \qquad (2)$$

where T is the temperature, k_b and h are the Boltzmann and the Planck constants, respectively. The computed activation energies are $E_A = 3.7$ Kcal mol^{-1}, $E_A = 3.5$ Kcal mol^{-1}, and $E_A = 2.2$ Kcal mol^{-1} for W_H-E, W_O-Alc, and W_H-Alc, respectively. A very close activation energy, $E_A = 3.5$ Kcal mol^{-1}, has been estimated for the water/solute H-bond in pentadecafluorooctanate (CsPFO) micelle.[40]

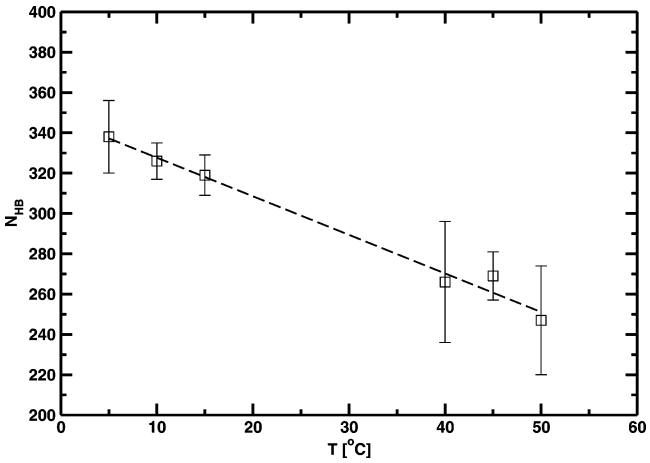

Figure 3. Number of water−water hydrogen bond nearby the oily core in function of temperature.

4. Water Structure around the Oil Core

Why does water in proximity of the oil core move away upon increasing the temperature? Surely, it is a consequence of the hydrophobic nature of the core; indeed, water molecules directly exposed to the hydrocarbon surface cannot bind to the surface and do not experience strong interactions such as those around the *E* units. Moreover, water in the proximity of the oily surface is expected to be structured differently compared to the bulk.

Many publications have been devoted in recent years to the characterization of water in contact with hydrophobic surfaces of different sizes[41−43] or in confined hydrophobic environments.[15−17] In open spaces, up to the nanoscale lengths, a weak dewetting is observed in the proximity of flat hydrophobic surface, on the contrary, the *clathrate-like* structure is characteristic of water around small hydrophobic molecules.[44] In the intermediate regime, typical, for example, of small hydrophobic patches in biological surfaces[9] or of grafted hydrophobic interfaces,[45] the arrangement of water molecules is more complex and depends on the topography of the solute surface. Recent simulations demonstrated also that the confinement inside nonpolar cavities and in carbon nanotubes forces water to assume ordered configurations[16,18] and intermediate ice/liquid structures,[17] respectively.

Our system provides an interesting model for the intermediate regime in a semi confined environment. The oily surface exposed to water, evaluated through the Voronoi analysis, results to be $\sigma \simeq 30$ nm^2 at $T = 10$ °C and $\sigma \simeq 28$ nm^2 at $T = 45$° C, but it is not uniformly distributed on the core surface. From the point of view of the water, the core surface, far from being a smooth spherical surface, appears to be a rough *urban map* where accessible patches (*roads*) are separated by regions screened by the hydrophilic fragments (*buildings*).

The structure of water around the hydrophobic patches and their connectivity will be then discussed in the following to elucidate the nature of the dehydration phenomena.

4.1. H-bonds Around the Oily Core. We consider a zone around the oily core rolling a sphere of radius $r = 4$ Å centered on each hydrocarbon atom. We select the water molecules inside this zone, and then we count the hydrogen bonds they form with other water molecules. In Figure 3 the number of hydrogen bonds evaluated around the oily surface is plotted as a function of the temperature. The decrease in temperature is linear with a slope of $\Delta N_{HB}/T = -1.91$ K^{-1}. Near the core from $T = 10$ to 45 °C the system loses ≃57 water−water H-bonds.

We can define the connectivity c as the ratio between the number of hydrogen bonds formed by the water molecules near

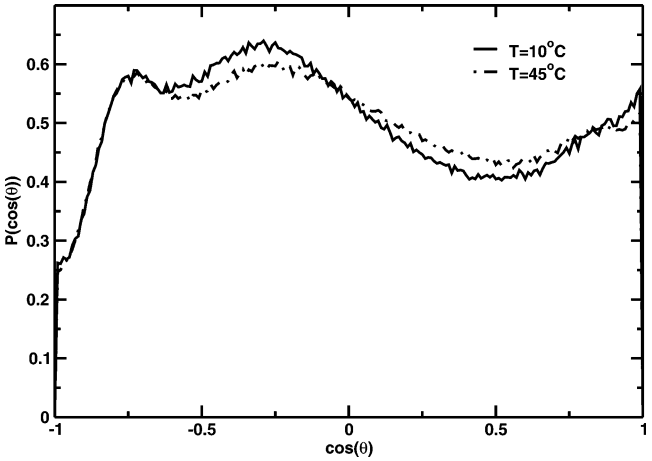

Figure 4. Distribution of the cos(θ) formed between the O−H bond of a water molecule and the local normal axis to the oily surface. The distributions are carried out for water molecules belong to the first hydration shell of the core. Data at temperature $T = 10$ °C (solid) and $T = 45$ °C (dotted−dashed) are compared.

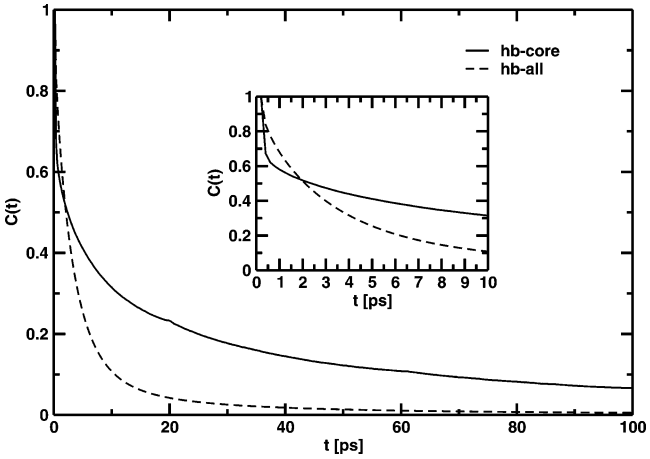

Figure 5. The correlation function $C(t)$ at $T = 10$ °C for the water−water hydrogen bond. With the solid line, the function is restricted to the water molecules near the oily core, while with the dashed line, the function is computed for all the solvent molecules in the system. In the inset, the correlation functions are plotted at short times.

the core and the total number of water molecules in contact with the core, $N_w = 158$ and $N_w = 136$ at $T = 10$ °C and $T = 45$ °C, respectively ($\Delta N_w = 22$). The temperature induces a variation of ≃4% in connectivity, from $c = 2.06$ ($T = 10$ °C) to $c = 1.98$ ($T = 45$ °C).[46] In a bulk system of water, upon increasing temperature from $T = 10$ °C to $T = 45$ °C, the same ratio c is evaluated from data obtained by independent simulations. The observed variation was ≃6%, thus the connectivity of the single water molecule around the core is slightly less sensitive to the increase of temperature than that of a bulk molecule. As a conclusion, the decrease in the number of hydrogen bonds is mainly caused by dehydration and not by a decrease in the connectivity.

Following the seminal paper of Cheng and Rossky,[9] we finally relate the described connectivities with the structural orientation of the water molecule. Through the distribution of the angle formed between the OH bond vector and the local normal axis to the core surface, defined as the vector connecting the hydrocarbon and the oxygen of the water molecule, it is indeed possible to discriminate between the clathrate-like structure and the *inverse* structure of water. In Figure 4 we show that water molecules around the oily exposed surface assumes, preferentially, a clathrate-like structure characterized by peaks around the value $\cos(\theta) = -0.34$ and $\cos(\theta) = 1$. High-temperature induces a broader distribution by enhancing the local disorder. However, a third peak around the value $\cos(\theta) \sim -0.74$ is also observed, this peak is reminiscent of the *inverse* structure and is not altered by temperature. This is probably due to the presence of a subset of water molecules which experience a stable inverse orientation.

The clathrate structure has been demonstrated to be stable in proximity of convex hydrophobic surfaces of protein, and is one of the possible structures assumed by water around flat patches.[9] In our system, the clathrate distribution does not change during the simulated trajectories, and water molecules tend in majority to partially cage the exposed hydrophobic groups.

4.2. H-bond Dynamics Near the Core Surface. We turn our attention to the dynamics of the water−water H-bond around the oily core by computing the correlation function $C(t)$ of eq 1 for those H-bonds involving water molecules in the interfacial volume spanned by our rolling sphere of 4 Å radius. $C(t)$ at temperature $T = 10$ °C is plotted in Figure 5. For the sake of comparison, we plot also the $C(t)$ computed for all water−water H-bonds in the solution. The $C(t)$s for the H-bonds around the core and for the entire solution are fitted with a double and a single-exponential function, respectively. The extracted lifetimes are reported in Table 2. Around the core, the $C(t)$ presents two time scales. At $T = 10$ °C, the fast decay has a characteristic time $\tau_1 = 6.9$ ps, 2 times larger than that of the entire solution, $\tau_1 = 3.7$ ps, which is shaped by bulk water−water hydrogen bond dynamics (indeed, the hydration water is 12% of the total solvent in the solution.) Thus the H-bonds are more stable around the core than in the bulk as has been observed in other simulations. For example in the case of a CsPFO micelle simulated at $T = 27$ °C, Balasubramanian, Pal, and Baghi[40] observed a delay of the 45% for the $C(t)$ computed near the micellar surface with respect to the bulk. A similar delayed dynamics has been detected by Xu and Berne for water around small hydrophobic regions of a polypeptide in water solution ($\tau = 6.8$ ps and =3.1 ps for the H-bonds around the hydrophobic amino acids and in bulk, respectively)[10] and by Li et al in the vicinity of a graphite-CH_3 surface ($\tau = 5.7$ ps).[11] The longer persistence of the water−water H-bonds around the hydrophobic regions is generally ascribed to the reduced number of neighbors which decreases the probability for a water molecule involved in a given H-Bond to switch partners. Thus the presence of the hydrophobic surface increases the free-energy barrier for breaking a water−water H-Bond.

The slow dynamics that we detect has a characteristic time $\tau_2 \simeq 80$ ps at $T = 10$ °C, and it has not been previously observed. This dynamics is not detectable if we consider the entire solution. Thus, our finding suggests that the water molecules upon breaking the formed H-bond at short time can reform it immediately. This is due to the semiconfined environment of the micellar interface that reduces the probability for a water molecule to leave the core surface. Actually, the correlation $\langle N_{w_{hb}}(t) N_{w_{hb}}(0)\rangle$, being $N_{w_{hb}}$ the number of water molecules involved in the hydrogen bonds counted in the hydration shell, has a characteristic time of 12 ps, larger than the lifetime $\tau_1 = 6.9$ ps. Increasing the temperature to $T = 45$ °C the lifetimes are half of those at $T = 10$ °C (see Table 2).

For times shorter than 1 ps, we observe that the $C(t)$ function decreases faster than that of the entire solution as is shown in the inset graph of Figure 5. This decay is due to the librational motion of the water molecules. As pointed out by Xu and Berne,

TABLE 2: Characteristic Times Extracted by Fitting the *C*(*t*) Correlation Function for Hydrogen-bond around the Oil Core and in the Entire Solution.[a]

hydrogen bond $T = 10$ °C	τ_1 [ps]	τ_2 [ps]
W−W (core)	6.9	80
W−W (all)	3.7	
hydrogen bond $T = 45$ °C	τ_1	τ_2
W−W (core)	3.2	44
W−W (all)	1.4	

[a] Note that for W−W around the core, the fit is performed using a double exponential. In the case of W−W for the all solution, a single exponential is used

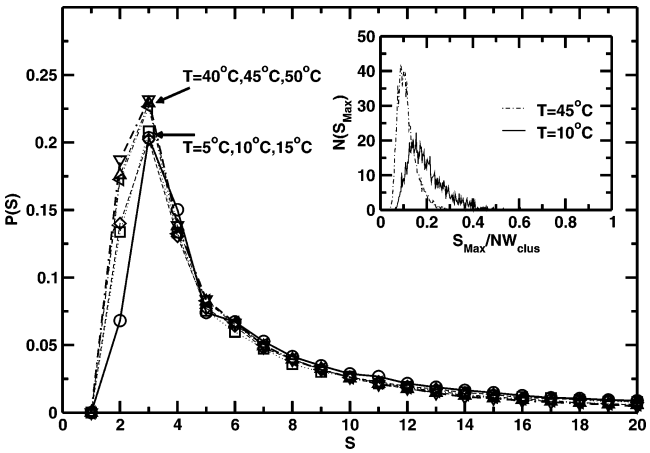

Figure 6. Probability distribution of the cluster size S at different temperatures. Symbols are as in Figure 1. In the inset graph, the histogram of the largest cluster size (S_{Max}) vs the ratio S_{Max}/N_{clus}, where N_{clus} is the number of water in clusters, is plotted for temperature $T = 10$ °C (in black) and $T = 45$ °C (with the dotted−dashed line).

TABLE 3: Characteristic Values of the Cluster Size Distribution at Different Temperatures

temperature	$\langle S \rangle$
$T = 5$ °C	10.6(1.2)
$T = 10$ °C	10.0(0.6)
$T = 15$ °C	9.3(0.3)
$T = 40$ °C	6.7(0.5)
$T = 45$ °C	6.9(0.2)
$T = 50$ °C	6.3(0.5)

this dynamic is critically dependent on the geometrical definition of the H-bond and depends on many body interactions, for these reasons, it is difficult to quantify the phenomenon. Xu and Berne observed, however, that for H-bonds around hydrophobic amino acids, the librational motion is slower than in the bulk while it is faster when the H-Bond is formed in proximity of charged ions Na^+. They speculated that the strong electric field generated by the ions induces rapid fluctuations between the broken and formed H-bond state. In our system the rupture of the H-bonds in the sub picosecond scale is really enhanced with respect to the entire solution (see inset graph of Figure 5), and following the indication of Xu and Berne, this can be related to the presence of the hydrophilic *E* units in proximity of the core surface.

4.3. Water Clusters on the Core Surface. Finally, we consider the H-bond network around the core surface by counting the clusters of hydrogen bonds spanning the oily core. A cluster is defined for each simulation frame as a set of water molecules all connected by H-bonds. The computed distribution of the cluster sizes for the simulated temperatures is plotted in Figure 6. The distributions are peaked around $S = 3$, and the tails extend to large values of the cluster size. The average cluster sizes $\langle S \rangle$ are computed and reported in Table 3. Note that the average cluster size decreases from $\langle S \rangle = 10.0(0.6)$ at $T = 10$ °C to $\langle S \rangle = 6.9(0.2)$ at $T = 45$ °C.

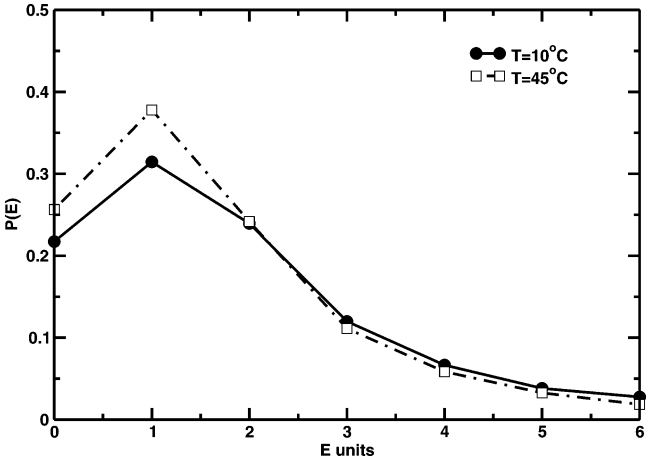

Figure 7. Probability distribution for a single cluster residing on the oil core to connect different *E* units: data at temperature $T = 10$ °C (solid line) and $T = 45$ °C (dotted−dashed line) are compared.

To gain insight in the structure of the clusters it is useful to consider the ratio r between the number of H-bonds and the number of molecules involved in the cluster: For an open network of N particles (either linear or branched structures), the ratio will be less than 1 ($r = (N - 1)/N$), while for closed structures as a ring, the r will be 1. More complex arrangements with molecules forming bridge connections inside the cluster will give a ratio $r > 1$. From our simulations $\langle r \rangle = 0.93$ and $\langle r \rangle = 0.87$ at $T = 10$ °C and $T = 45$ °C, respectively, thus a linear or branched connection is expected for the clusters.

We look at the distribution of the maximum cluster size vs the ratio S_{Max}/N_{clus}, where N_{clus} is the average number of water molecules belonging to clusters and S_{Max} is the size of the largest cluster computed in each simulation frame. The results are plotted in the inset graph of Figure 6. The distributions indicate that our system is well below the percolation threshold for which the maximum is expected to be close to 1.[47] Thus the H-bond network does not connect all the exposed hydrophobic patches of the core surface. Similar profiles have been reported recently for a low hydrated lysozyme system.[13]

As expected, the cluster analysis shows that, upon increasing the temperature, dehydration induces a reduction of the cluster extension. However, it is interesting to understand how the clusters change their distribution on the core surface and how this is related to the distribution of the hydrophilic units on the surface. The probability for a single cluster to connect different hydrophilic units P(*E*) is then computed (see Figure 7). By increasing the temperature, the probability to connect more then two units decreases from the 45% to the 38%, in turn the probability to concentrate a cluster around a single hydrophilic unit, P(1), or to find an isolate cluster, P(0), increases with temperature. These information suggest that the water molecules, escaping from the core surface upon raising the temperature, break the connectivity of the clusters which remain localized around the hydrophilic units or isolated on the core surface. This is clearly related to the distribution of the polar *E* units anchorage on the core surface that is modified by the temperature raise.[5]

From the average cluster size and the covering surface of a single water molecule ($\simeq$14 Å^2) we can roughly estimate the average extension of the single hydrophobic patch exposed to

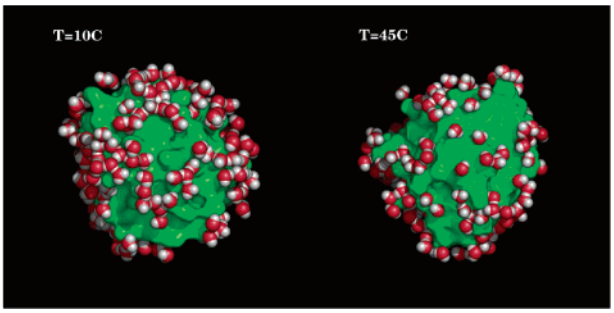

Figure 8. Pictorial view of the water clusters spanning the oily core surface of the micelle (green) at temperatures $T = 10$ °C and $T = 45$ °C.

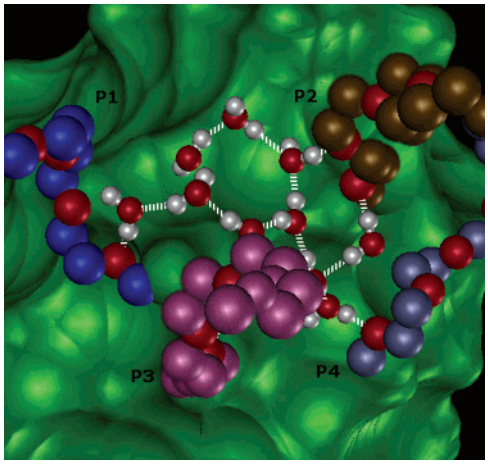

Figure 9. A branched network of water molecules spanning the oil core (green surface) and connecting several hydrophilic fragments (P_1 in blue, P_2 in brown, P_3 in magenta, and P_4 in light blue). The oxygens of the *E* units are colored in red. Water is in ball-and-stick. The hydrogen bonds are represented by dashed white lines. The picture is extracted from a simulation at $T = 10$ °C.

water: 1.4 nm^2 at $T = 10$ °C and 1 nm^2 at $T = 45$ °C. These values are comparable to the estimated extension of the hydrophobic regions in protein surfaces, and this further confirms that our model provides useful information for biosystems such as proteins. A pictorial view of the spanning clusters at different temperatures is presented in Figure 8. In Figure 9, we report also a typical structure of a water cluster on the core surface, the branched network spans the oily core and connects several hydrophilic fragments.

5. H-Bond Water Network along the Interface

Following the shell analysis framework,[5] we have studied the cluster size in the radial shells along the interface. In Figure 10, the average cluster size is plotted as a function of the shell edge for the temperatures $T = 10$ °C and $T = 45$ °C. First, we remark that at $T = 10$ °C in the first shell, the cluster size has the highest value, $\langle S \rangle = 16$ molecules. A plateau around the value $\langle S \rangle = 6$ is then observed for the intermediate shells, $i = 2, 3, 4, 5$. In the external shell, in which water is closer to the bulk phase, the average cluster size increases again. To take into account that the amount of water in a shell varies along the interface and it also depends on temperature, we report in the inset of Figure 10 the average cluster size normalized with the corresponding number of water molecules $\langle S \rangle / N_w$(shell). This quantity exhibits very minor temperature dependence everywhere along the interface but in the first hydration shell where it takes the values $\langle S \rangle / N_w = 0.87$ at $T = 10$ °C and $\langle S \rangle / N_w = 0.73$ at $T = 45$ °C. Thus upon increasing temperature, not only

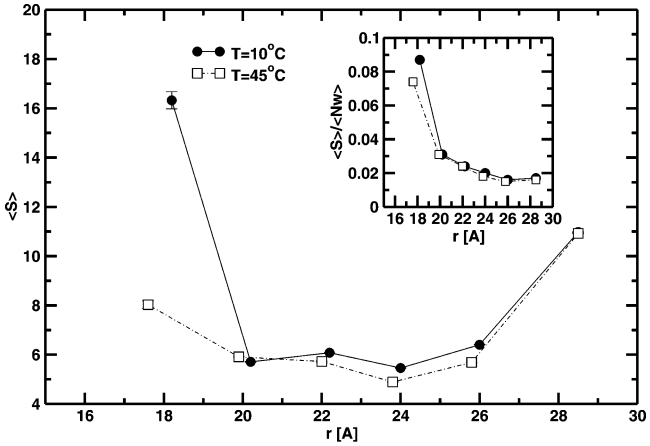

Figure 10. Average cluster size computed for water inside radial shells. Data at temperature $T = 10$ °C (solid line) and $T = 45$ °C (dotted−dashed line) are compared. In the inset graph, the average cluster size is normalized with respect the amount of water contained in each shell.

the number of molecules in the inner hydration shell decreases, but also the probability for one molecule to participate in a cluster. However, the probability of a water molecule to participate in a cluster is higher for the internal shell at both temperatures, and this shows how water molecules privilege to form H-bond-connected structures in proximity of the core.

6. Conclusion

Dehydration of a $C_{12}E_6$ spherical micelle upon increasing temperature is characterized through the statistics and dynamics of individual H-bonds formed by water in the system, and specific attention is devoted to the water−water hydrogen bonds network within the micellar interface. As highlighted in a previous study, dehydration, measured through the shell analysis, occurs in the internal part of the micellar interface. Moreover, the number of water molecules hydrating the oil core and the hydrophilic units both decreases as effect of the increase of temperature, but the percentage change is found to be larger and significant for the hydration shell of the oil core only. Upon raising the temperature from $T = 10$ °C to $T = 45$ °C, the total number of H-Bond formed by water and the *E* units decreases from 310 to 297 ($\Delta N_{hb} = 13$, 4%) and the distribution of such H-bonds along the hydrophilic fragments changes as well. On the contrary, in the vicinity of the oil core surface, the water molecules can form H-bonds only among themselves. Thus in this region we analyzed the number of H-bonds formed among water molecules and its variation with temperature. The system loses roughly 57 H-bonds raising the temperature from $T = 10$ °C to $T = 45$ °C (17%) as consequence of dehydration.

The persistence of a water−water H-bond on the oily core exhibits an interesting relaxation characterized by two time scales, both slower than the characteristic time of the entire solution. At $T = 10$ °C, the fast decay has a characteristic time of $\tau_1 = 6.9$ ps, a value close to that computed in other systems such as peptide/water solution ($\tau = 6.8$ ps) and graphite-CH_3/water interface ($\tau = 5.7$ ps). The slower decay, $\tau_2 = 80$ ps at $T = 10$ °C and 44 ps at $T = 45$ °C, has not been detected in other micellar systems, and it is a specific consequence of the confinement around the core that reduces the probability for water molecules to leave the core. These two time scales can be ascribed to the presence of a fast dynamic related to orientational changes and a slow dynamic due to the escaping of water molecules from the hydration shell. If this second process is slow enough, then recombining phenomena could

occur, and the same H-bond can be reconstructed. That is, two water molecules on the core surface can break and recombine their common H-bond, due to rotational mismatching and rematching, before the specific water molecules leave the core surface. At time shorter than 1 ps, the H-bonds around the core are characterized by high librational motion probably induced by the presence of the hydrophilic units in the hydration shell of the core.

Water around the core forms linear or branched networks whose extensions change with temperature. The cluster analysis shows that the hydrophobic patches exposed to water are not fully connected by the water networks spanning the surface and the system appears to be below the percolation threshold. The coverage of the oily core by water decreases upon increasing temperature, and this further reduces the connection between the hydrophobic patches. This can be related to the rearrangement of the hydrophilic moieties in the interface, which modifies the distribution of screened regions (or polar sites) on the core. At high temperature, the clusters are more localized around a single hydrophilic unit or are isolated on the core, thus their capability to connect several units decreases with dehydration. The average size of the hydrophobic patches is estimate to be around 1 nm^2, very close to the estimates for protein surfaces.

Following a suitable separation of the interface in concentric hydration shells, an important reduction of the cluster size upon increasing T is observed mainly in the inner part of the interface. In the innermost shell we observe also the largest cluster size which shows a strong structural effect due to the confinement on the core. In the middle part, $E = 2, 3, 4, 5$, the cluster extension has the lower value, signing the structural breaking role of the hydrophilic fragments.

In conclusion, our results show that by increasing the temperature, the dehydration of spherical micelle of $C_{12}E_6$ is accompanied by significant structural changes of the water layer solvating the oily core; this has been detected by computing the size and distribution of the water−water H-bond networks. Conversely, properties of the single molecule like the connectivity, the local orientation, and the HB-bond lifetime do not manifest any specific contribution to the dehydration, being the change with temperature comparable to that induced in a bulk of water.Thus the dehydration is basically related to a collective reorganization of the water−water H-bond network on the core. We also demonstrated how these collective structures are related to the confining effect caused by the long hydrophilic fragments.

Acknowledgment. F.S. thanks Andrea Pagnani for useful discussion and help provided in the development of the cluster analysis and Peter J. Rossky for the interesting discussions.

References and Notes

(1) Carlström, G.; Halle, B. *J. Chem. Soc., Faraday Trans. 1* **1989**, *85*, 1049.

(2) Jonströmer, M.; Jonsson, B.; Lindman, B. *J. Phys. Chem.* **1991**, *95*, 3293.

(3) Romsted, L. S.; Yao, J. *Langmuir* **1996**, *12*, 2425.

(4) Romsted, L. S.; Yao, J. *Langmuir* **1999**, *15*, 326.

(5) Sterpone, F.; Briganti, G.; Marchi, M.; Pierleoni, C. *Langmuir* **2004**, *20*, 4311.

(6) Karlström, G. *J. Phys. Chem.* **1985**, *89*, 4962.

(7) Ahlnäs, T.; Karlström, G.; Lindman, B. *J. Phys. Chem.* **1987**, *91*, 4030.

(8) Lijnzaad, P.; Berendsen, H.; Argos, P. *Proteins* **1996**, *26*, 192.

(9) Cheng, Y. K.; Rossky, P. J. *Nature* **1998**, *392*, 696.

(10) Xu, H.; Berne, B. J. *J. Phys. Chem. B* **2001**, *105*, 11929.

(11) Li, J.; Liu, T.; Li, X.; Ye, L.; Chen, H.; Fang, H.; Wu, Z.; Zhou, R. *J. Phys. Chem B* **2005**, *109*, 13639.

(12) Koishi, T.; Yoo, S.; Zeng, X.; Narumi, T.; Sasukita, R.; Kawai, A.; Furusawa, H.; Suenaga, A.; Okimoto, N.; Futatsugi, N.; Ebisuzaki, T. *Phys. Rev. Lett.* **2004**, *93*, 18701.

(13) Oleinikova, A.; Smolin, N.; Brovchenko, I.; Geiger, A.; Winter, R. *J. Phys. Chem. B* **2005**, *109*, 1988.

(14) Oleinikova, A.; Brovchenko, I.; Smolin, N.; Geiger, A. K. A.; Winter, R. *Phys. Rev. Lett.* **2005**, *95*, 247802.

(15) Vaitheeswaran, S.; Rasaiah, J. C.; Hummer, G. *J. Chem. Phys.* **2004**, *121*, 7955.

(16) Vaitheeswaran, S.; Yin, H.; Rasaiah, J. C.; Hummer, G. *Proc. Natl. Acad. Sci. U.S.A.* **2004**, *101*, 17002.

(17) Mashl, R. J.; Joseph, S.; Aluru, N. R.; Jakobsson, E. *Nano Lett.* **2003**, *3*, 589.

(18) Yoshizawa, M.; Kusakawa, T.; Kawano, M.; Ohhara, T.; Tanaka, I.; Kurihara, K.; Niimura, N.; Fujita, M. *J. Am. Chem. Soc.* **2005**, *127*, 2798.

(19) Sterpone, F.; Briganti, G.; Pierleoni, C. *Langmuir* **2001**, *17*, 5103.

(20) Tasaki, K. *J. Am. Chem. Soc.* **1996**, *118*, 8459.

(21) MacKerell, A., Jr.; Bashford, D.; Bellot, M.; Dunbrack, R., Jr.; Evanseck, J.; Field, M.; Fischer, S.; Gao, J.; Guo, H.; Ha, S.; Joseph-McCarthy, D.; Kuchnir, L.; Kuczera, K.; Lau, F.; Mattos, C.; Michnick, S.; Ngo, T.; Nguyen, D.; Prodhom, B.; W. R., III; Roux, B.; Schlenkrich, M.; Smith, J.; Stote, R.; Straub, J.; Watanabe, M.; Wiorkiewicz-kuczera, J.; Yin, D.; Karplus, M. *J. Phys. Chem. B* **1998**, *102*, 3586.

(22) Tobias, D. J.; Tu, K.; Klein, M. L. *J. Chim. Phys.* **1997**, *94*, 1482.

(23) Tobias, K. T. D. J.; Klein, M. L. *J. Phys. Chem.* **1995**, *99*, 10035.

(24) Ryckaert, J. P.; Ciccotti, G.; Berendsen, H. J. C. *J. Comput. Phys.* **1977**, *23*, 327.

(25) Melchionna, S.; Ciccotti, G. *J. Chem. Phys.* **1997**, *106*, 195.

(26) Essmann, U.; Perera, L.; Berkowitz, M. L.; Darden, T.; Lee, H.; Pedersen, L. G. *J. Chem. Phys.* **1995**, *103*, 8577.

(27) Pal, S.; Balasubramanian, S.; Bagchi, B. *Phys. Rev. E* **2003**, *67*, 061502.

(28) Pal, S.; Balasubramanian, S.; Bagchi, B. *J. Phys. Chem. B* **2003**, *107*, 5194.

(29) Harris, J. M. In *Poly(ethylene glycol) Chemistry*; Harris, J. M., Ed.; Plenum: New York, 1992.

(30) Maxfield, J.; Shepherd, I. *Polymer* **1972**, *16*, 505.

(31) Bekiranov, S.; Bruinsma, R.; Pincus, P. *Phys. Rev. E* **1997**, *55*, 577.

(32) Heymann, B.; Grübmuller, H. *Chem. Phys. Lett.* **1999**, *307*, 425.

(33) Bandyopadhyay, S.; Tarek, M.; Lynch, M. L.; Klein, M. L. *Langmuir* **2000**, *16*, 942.

(34) Zheng, J.; Li, L.; Chen, S.; Jiang, S. *Langmuir* **2004**, *20*, 8931.

(35) Allen, R.; Bandyopadhyay, S.; Klein, M. L. *Langmuir* **2000**, *16*, 10547.

(36) Sterpone, F.; Marchetti, G.; Pierleoni, C.; Marchi, M. *J. Phys. Chem. B* **2006**, *110*, 11504.

(37) In our analysis, we use a well-established geometrical criteria in order to detect the H-bonds formed by a donor and an acceptor: the distance between the donor and the acceptor must be inferior to 3.5 Å and the angle formed by the donor−acceptor axis and the donor-hydrogen bond inferior to 30°. The radial cutoff is appropriate for either water−water or water−PEO H-bonds as can be inferred by the study of the pair-correlation functions.[19,20,39] The angular cutoff has been demostrated to be, at some extent, equivalent to an energetic criteria.[28]

(38) Upon raising the temperature from $T = 10$ °C to $T = 45$ °C, the gauche states of the OC torsion increase of about 4%, whereas the population distribution of the CC torsion does not change (94.6% gauche$^+$, 5.4% trans).

(39) Luzar, A.; Chandler, D. *Nature* **1996**, *379*, 55.

(40) Balasubramanian, S.; Pal, S.; Bagchi, B. *Phys. Rev. Lett.* **2002**, *89*, 115505.

(41) Lum, K.; Chandler, D.; Weeks, J. D. *J. Phys. Chem. B* **1999**, *103*, 4570.

(42) Huang, X.; Margulis, C. J.; Berne, B. J. *J. Phys. Chem B* **2003**, *107*, 11742.

(43) Huang, X.; Margulis, C. J.; Berne, B. J. *Proc. Natl. Acad. Sci. U.S.A.* **2003**, *100*, 11953.

(44) Blokzijl, W.; Engberts, J. B. F. N. *Angew. Chem., Int. Ed. Eng.* **1993**, *32*, 1545.

(45) Ashbaugh, H. S.; Pratt, L. R.; Paulaitis, M.; Clohecy, J.; Beck, T. L. *J. Am. Chem. Soc.* **2005**, *127*, 2808.

(46) We alert the reader that the numbers of water molecules in contact with the core are different from those given in ref 5 because we use a different definition of the contacts. In the previous work, the Voronoi contact between the oily surface and water was used, here we consider a shell based on a cutoff radius.

(47) Stauffer, D.; Aharon, A. *Introduction to Percolation Theory*; Taylor & Francis: London, 1994.